Dual Carrier Modulation to Overcome Dispersion Power Fading (DPF) in Radio Over Fiber (ROF) Systems

Febrizal Ujang[1], Muhammad Firdaus[2], Ken Paramayudha[3] and Teguh Firmansyah[4]

[1,2]Department of Electrical Engineering. Universitas Riau, Pekanbaru, Indonesia
[3]Research Center for Telecommunication, National Research and Innovation Agency (BRIN), Bandung, Indonesia [4]Department of Electrical Engineering, Universitas Sultan Ageng Tirtayasa, Cilegon, Banten, 42435, Indonesia.
febrizal@eng.unri.ac.id, muhammad.firdaus0625@student.unri.ac.id, ken.paramayudha@brin.go.id, teguhfirmansyah@untirta.ac.id

Abstract: In Radio over Fiber (RoF) systems, when an optical carrier is intensity-modulated by a radio frequency (RF) signal, the resulting optical spectrum contains a double sideband structure. As this signal propagates through a dispersive fiber link, chromatic dispersion causes variations in the recovered RF power. This effect, commonly identified as dispersion power fading (DPF), manifests as fluctuations in the RF output signal strength. Several approaches, such as Optical Single Sideband (OSSB) modulation, have been employed to mitigate DPF. However, these techniques typically involve transmitter designs of considerable complexity. To address this issue, this paper introduces a new approach called Dual Carrier Modulation (DCM). In DCM, the RF signal is imposed onto the optical signal through the use of two laser diodes. The emission from the first diode is then combined with that of the second diode, which is tuned so that its optical frequency corresponds to the carrier frequency offset by the RF signal frequency. In the RoF system with direct modulation given RF signal input with frequencies of 60, 40, and 30 GHz, large power fluctuations occur, with C/N deviation factor values of 7.59, 7.63, and 6.30, respectively. In contrast, in the RoF system using the DCM method under the same RF frequencies, the C/N deviation factor values are significantly reduced to 0.05, 0.20, and 0.47, indicating that DCM can effectively mitigate DPF.

Keywords: Chromatic Dispersion, Direct Modulation, Radio Over Fiber, Dual Carrier Modulation, Dispersion Power Fading

1. Introduction

A system called Radio over Fiber (RoF) has been developed to allow radio frequency (RF) signals to be carried over optical fiber. This is achieved by modulating an optical carrier with the RF signal during transmission. At the Base Station (BS), an electro-optic (E/O) converter is employed to translate the RF signal into its optical form. The optical signal is then delivered to the Radio Access Point (RAP), where an opto-electronic (O/E) converter restores it to the RF domain. From the RAP, the regenerated RF signal is propagated over the air to the Mobile Station (MS). Optical sources may be modulated using either direct or external methods. At the receiver side, extracting the RF signal from intensity modulation (IM) is known as Direct Detection (DD), while retrieval from phase modulation is referred to as coherent detection [1, 2].

The optical double sideband (ODSB) format produces a spectrum containing two sidebands—upper and lower—distributed on either side of the carrier frequency. Such a signal arises when an RF signal is used to intensity-modulate an optical wave. During transmission through an optical fiber, chromatic dispersion causes the carrier and sideband components to travel at different relative velocities. As a result, by the time the modulated signal reaches the receiver, a phase shift φ develops between the optical carrier and the sidebands. The phase shift φ is determined by the RF modulation frequency (f_m), fiber length (L), and the operating wavelength. Consequently, during opto-electronic (O/E) conversion, two identical RF components are generated with a relative phase offset of 2φ. The superposition of these components results in alternating signal reinforcement and cancellation in the recovered RF

Received: May 9th, 2024. Accepted: September 23rd, 2025
DOI: 10.15676/ijeei.2025.17.3.4

signal, a phenomenon referred to as dispersion power fading (DPF) [3]. Sideband cancellation effects, leading to significant power loss, occur when $\varphi = \pi/2$ [4].

In [5], the use of the irregular θ method is investigated as a means to mitigate dispersion power fading (DPF) in Radio over Fiber (RoF) links, where a dual-drive Mach–Zehnder modulator (DD-MZM) serves as the electro-optic (E/O) converter. The results show that the irregular θ method achieves superior mitigation of dispersion fading compared to the OSSB modulation scheme across all tested modulation indices (m). Furthermore, RoF links using the irregular θ technique exhibit effective suppression of dispersion fading for $m \leq 1$, while maintaining a consistent deviation factor (DF) regardless of RF frequency and optical wavelength. These findings highlight the irregular θ method as a promising solution for enhancing the reliability and efficiency of RoF systems.

In [6], a broadband microwave photonic mixer is proposed to support fiber transmission without DPF. The proposed configuration is implemented using a dual-parallel dual-polarization Mach–Zehnder modulator (DP-DPMZM). A continuous-wave (CW) signal generated by a distributed-feedback laser diode (DFB-LD) is simultaneously modulated by the intermediate frequency (IF)/RF and local oscillator (LO) signals using the DP-DPMZM. To accomplish this, the IF/RF signal is divided by a phase shifter (PS), while the LO signal is separated into two branches by means of a 90° electrical hybrid coupler (HC). The resulting signals are applied to the four sub-MZMs within the DP-DPMZM which are all biased at their minimum transmission levels in order to generate carrier-suppressed double-sideband (CS-DSB) modulation. With this configuration, the microwave photonic mixer enables 20 km fiber transmission free from DPF. Moreover, it provides continuously adjustable phase shifts greater than 360° in the frequency range spanning from 0.1 GHz to 29.9 GHz, while maintaining power variations during phase tuning below 4 dB.

One approach to mitigating DPF is carrier phase shifting (CPS) [7]. In this method, the optical carrier phase (φ) is pre-compensated prior to transmission so that, after traveling through the fiber, φ becomes zero. This guarantees that the recovered RF signal remains in a constructive interference condition. The drawback of this approach is that φ needs to be pre-tuned based on the fiber length (L), the RF frequency (f_m), and the optical carrier wavelength (λ_c), since it is directly dependent on these factors.

Another approach to mitigating DPF is to transform the modulated optical spectrum into the Optical Carrier Suppressed (OCS) form [8-10]. Optical Carrier Suppression (OCS) can be viewed as a form of ODSB modulation where the optical carrier is eliminated, resulting in only the upper and lower sidebands remaining. In this approach, the resulting RF signal comes from the beating between the two sidebands, thereby eliminating the interference responsible for DPF. However, a limitation of this method is that the frequency of the recovered RF signal becomes twice that of the transmitted RF signal, thereby making down-conversion at the receiver essential for reconstructing the signal at its fundamental frequency.

DPF can also be mitigated by employing the Optical Single Sideband (OSSB) modulation technique [11]. In this approach, the spectrum is characterized by the presence of the optical carrier and just one sideband, either upper or lower. Thus, the OSSB approach ensures that only one RF signal with the same frequency as the transmitted RF signal is generated at the receiver, eliminating the need to perform down-conversion at the receiver. A Dual-Drive Mach–Zehnder Modulator (DD-MZM) biased at the quadrature point, with a 90° phase shift (θ) between the two RF drive signals, can be employed to realize OSSB modulation [12]. The OSSB modulation scheme generated in this way requires a complex transmitter circuit. Considering this, in this study, we propose the dual-carrier modulation (DCM) method, which overcomes the complexity of OSSB modulation by enabling a simpler implementation using only two directly modulated lasers, while effectively mitigating DPF.

2. Methods

A. Direct Modulation in Radio Over Fiber System

An RF signal can modulate an optical carrier in two ways: the first is direct modulation of the optical source, such as laser diodes (LDs) or light-emitting diodes (LEDs) [13]; the second is external modulation of a pre-generated optical signal.. Each of these techniques allows for modulation of the optical carrier in terms of amplitude (intensity/power) and phase [14, 15]. The modulation scheme of the ROF channel with direct IM can be seen in Figure 1. Within direct IM, modulation is achieved by altering the laser diode's bias/ drive current proportionally to the applied RF signal, causing the light intensity produced to vary according to the modulating RF signal. This technique results in the generation and modulation of light occurring in a single step.

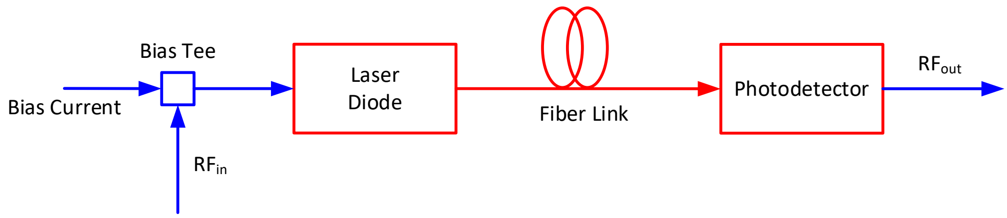

Figure 1. Radio Over Fiber (ROF) Direct Modulation Scheme

In the context of RoF transmission, dispersion in the optical fiber results in diminished retrieved RF power, a phenomenon identified as dispersion power fading (DPF). The phenomenon of DPF in RoF links may be effectively visualized through the spectral evolution illustrated in Figure 2. As shown in Figure 2a, modulating an optical carrier (f_c) with an RF signal (f_m) via direct modulation technique, the resulting optical spectrum is in the form of double sideband (DSB). The modulated optical signal can be expressed in exponential form, as shown in Equation (1) [2].

$$E_1(t) = \frac{m}{2} e^{j2\pi(f_c - f_m)t} + e^{j2\pi f_c t} + \frac{m}{2} e^{j2\pi(f_c + f_m)t} \quad (1)$$

where m is the modulation depth of the laser.

When transmitted through a dispersive link, the signal's components propagate at unequal velocities. This variation causes a phase difference, represented by ϕ, to arise between the optical carrier (OC) and its sidebands, as illustrated in Figure 2b. The value of ϕ satisfies Equation 2 [2].

$$\phi = \frac{DL\lambda_c^2 f_m^2}{c} \quad (2)$$

Where D is the chromatic dispersion coefficient of the fiber, L is the fiber length, c is the speed of light in a vacuum, and λ_c is the optical wavelength. At the receiver, the signal can be formulated as shown in Equation (3):

$$E_{rx1}(t) = \frac{m}{2} e^{j2\pi(f_c - f_m)t} + e^{j2\pi f_c t} . e^{j\phi} + \frac{m}{2} e^{j2\pi(f_c + f_m)t} . e^{j4\phi} \quad (3)$$

$$E_{rx1}(t) = \frac{m}{2} e^{j2\pi(f_c - f_m)t} + e^{j(2\pi f_c t + \phi)} + \frac{m}{2} e^{j(2\pi(f_c + f_m)t + 4\phi)} \quad (4)$$

Once the optical signal reaches the photodetector (PD), it produces two RF signals, as illustrated in Figure 2c. Since the PD acts as a squared-envelope operator, it produces a signal that satisfies the following equation:

$$|E_{rx1}(t)|^2 = E_{rx}(t). E^{*}{}_{rx}(t)$$

$$|E_{rx1}(t)|^2 = \left\{\frac{m}{2} e^{j2\pi(f_c - f_m)t} + e^{j(2\pi f_c t + \phi)} + \frac{m}{2} e^{j(2\pi(f_c + f_m)t + 4\phi)}\right\} . \left\{\frac{m}{2} e^{-j2\pi(f_c - f_m)t} + e^{-j(2\pi f_c t + \phi)} + \frac{m}{2} e^{-j(2\pi(f_c + f_m)t + 4\phi)}\right\} \quad (4)$$

Since the desired signal corresponds only to the frequency f_m , it can be extracted as:

$$|E_{rx1}(t)|^2 = \left(\frac{m}{2}\right) e^{j(2\pi f_m t + \phi)} + \left(\frac{m}{2}\right) e^{j(2\pi f_m t + 3\phi)}$$

$$|E_{rx1}(t)|^2 = e^{j2\pi f_m t} \left\{\left(\frac{m}{2}\right) e^{j\phi} + \left(\frac{m}{2}\right) e^{j3\phi}\right\} \quad (5)$$

The current produced at the PD can be expressed as the real part of Equation (5), thus

$$X_{rec1}(t) = \left\{\left(\frac{m}{2}\right)e^{j\phi} + \left(\frac{m}{2}\right)e^{j3\phi}\right\}\cos 2\pi f_m t \quad (6)$$

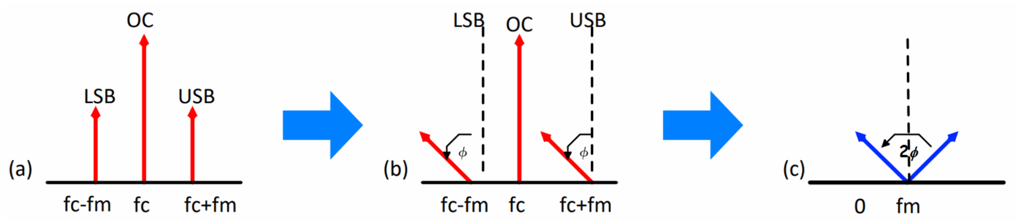

Figure 2. Optical signal evolution along the ROF link with direct modulation' (a) modulated optical signal (output of the Direct Modulator), (b) optical signal at the receiver (before detection), and (c) RF signal after detection (output of the photodetector, PD).

RF signal I is produced by the interaction between the lower sideband (LSB) and the optical carrier (OC), whereas RF signal II is produced by the interaction between the upper sideband (USB) and the OC [2]. Although both signals have equal amplitudes, they differ in phase by 2ϕ. The output RF signal power of the PD can be expressed as the square of the amplitude factor obtained from Equation (6), so the amount of RF signal power generated by the PD at fiber length L is

$$P_{rec1}(L) = \left\{\left(\frac{m}{2}\right)e^{j\phi} + \left(\frac{m}{2}\right)e^{j3\phi}\right\}^2 \quad (7)$$

Since the value of ϕ is determined by the D, L, λ_c and f_m, when D, λ_c and f_m, are held constant, DPF occurs as L changes, causing fluctuations in the received RF signal. When ϕ reaches 90°, the two RF signals become out of phase, causing them to cancel each other out. As a result of this cancellation, the RF signal power experiences a substantial decline, a condition referred to as deep fading.

Reduction of the RF signal power at the photodetector output induced by fiber dispersion constitutes the carrier-to-noise (C/N) penalty. Evaluation of the penalty involves contrasting the received power $P_{rec}(L)$ through the fiber with the received power without the fiber link [4]. To examine DPF in the RoF system, Equation (7) is applied to calculate the signal power using the parameters: c = 3.10^{-8} m/s, λ_c = 1550 nm, D = 17 ps/(nm.km), m = 0.2 and f_m = 60 GHz. The computation is performed for fiber lengths (L) ranging from 0 to 5 km, with increments of 0.1 km. The results of this calculation are then used to plot the C/N penalty curve as can be seen in Figure 3.

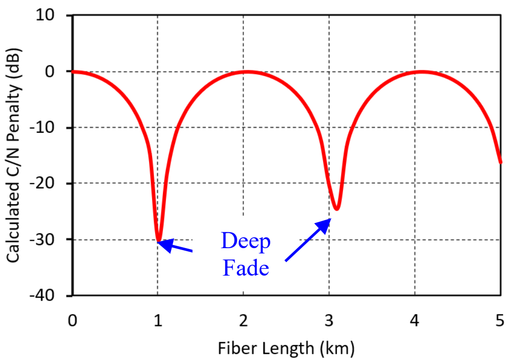

Figure 3. C/N Penalty curve calculated for RoF system with direct optical modulation technique.

From the C/N penalty curve, it can be observed that, for fiber lengths between 1 and 5 km, the RF signal power detected by the PD fluctuates, with deep fades occurring at 1 km and 3.1 km. The level of RF signal power fluctuation in RoF systems is quantified by the C/N deviation factor [5], where a larger value indicates poorer system performance. A system is considered ideal when this factor approaches zero. For this system, the C/N deviation factor was measured as 7.59, indicating that the RoF system with direct optical modulation exhibits poor performance.

B. Dual Carrier Modulation

To suppress dispersion power fading, Dual Carrier Modulation (DCM) has been developed as an alternative modulation scheme by carrying the modulating signal (RF signal) using two OCs with a frequency difference equal to the modulating signal frequency. DCM method can be generated using both direct and external modulation techniques. In this study, direct modulation technique is used to implement this method.

Figure 4 illustrates the RoF circuit employing the DCM technique, where the transmission link is composed of a Transmitter, Channel, and Receiver. The Transmitter consists of the output of LD_1 with a frequency of f_c combined with the output of LD_2 with a frequency of f_c+f_m. The optical carrier signals generated by LD_1 and LD_2 are each modulated by RF signals with a frequency of f_m. The channel in this RoF link is an optical fiber that is dispersive, while the Receiver section employs a PD to recover the electrical signal.

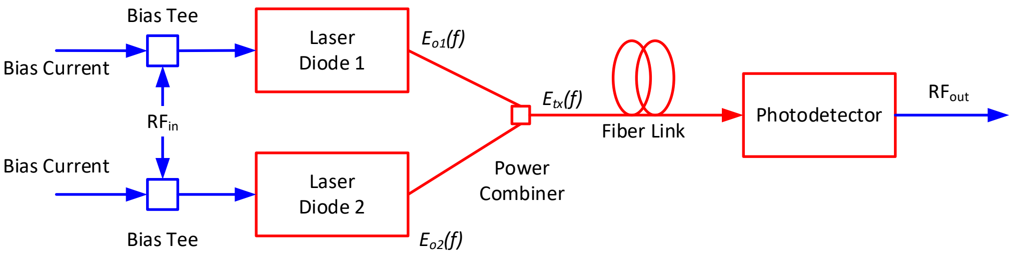

Figure 4. Link RoF with Dual Carrier Modulation

When an optical carrier at frequency f_c is modulated by a signal of frequency f_m, the resulting modulated optical signal I exhibits the spectrum illustrated in Figure 5a and follows Equation (1). When the optical carrier at frequency f_c+f_m is modulated by the signal at frequency f_m, it produces the modulated optical signal II, whose spectrum is illustrated in Figure 5b and is described by Equation (8).

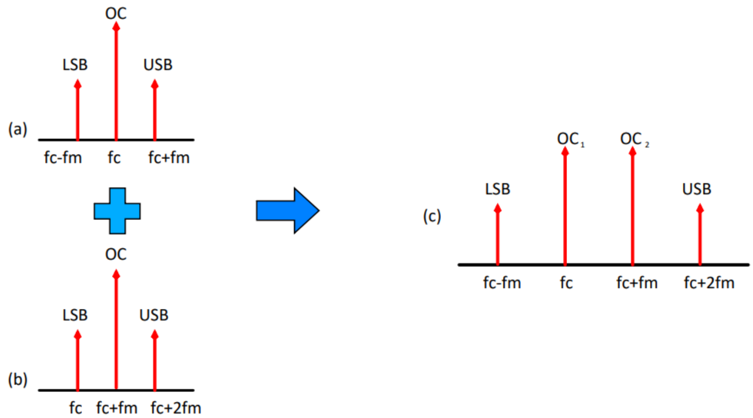

Figure 5. DCM signal formation process, (a) modulated optical signal I, (b) modulated optical signal II, and (c) the sum of optical signals I and II (DCM optical signal).

$$E_2(t) = \frac{m}{2} e^{j2\pi f_c t} + e^{j2\pi(f_c+f_m)t} + \frac{m}{2} e^{j2\pi(f_c+2f_m)t} \tag{8}$$

To generate DCM, modulated optical signal I is combined with modulated optical signal II using a power combiner, forming an optical signal with a spectrum as shown in Figure 5c, which satisfies Equation 9.

$$E_{tx}(t) = E_1(t) + E_2(t)$$
$$E_{tx}(t) = \frac{m}{2} e^{j2\pi(f_c-f_m)t} + \left(\frac{m}{2}+1\right) e^{j2\pi f_c t} + \left(\frac{m}{2}+1\right) e^{j2\pi(f_c+f_m)t} + \frac{m}{2} e^{j2\pi(f_c+2f_m)t} \quad (9)$$

The working principle of the DCM method in overcoming DPF can be explained through Figure 6. When the DCM signal in Figure 6a passes through the dispersive link, a relative phase difference between OC_1 and OC_2, LSB dan USB occurs as seen in Figure 6b. The optical signal arriving at the receiver will fulfill the equation (10):

$$E_{rx2}(t) = \frac{m}{2} e^{j2\pi(f_c-f_m)t} + \left(\frac{m}{2}+1\right) e^{j2\pi f_c t}. e^{j\phi} + \left(\frac{m}{2}+1\right) e^{j2\pi(f_c+f_m)t}. e^{4j\phi} + \frac{m}{2} e^{j2\pi(f_c+2f_m)t}. e^{j9\phi}$$
$$E_{rx2}(t) = \frac{m}{2} e^{j2\pi(f_c-f_m)t} + \left(\frac{m}{2}+1\right) e^{j(2\pi f_c t+\phi)} + \left(\frac{m}{2}+1\right) e^{j(2\pi(f_c+f_m)t+4\phi)} + \frac{m}{2} e^{j(2\pi(f_c+2f_m)t+9\phi)} \quad (10)$$

When the photodetector (PD) detects this signal, it will result in 3 different RF signals with spectra as shown in Figure 6c.

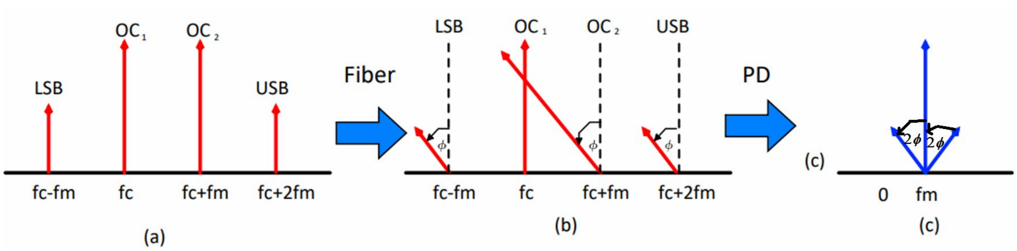

Figure 6. Evolution of optical signals along the ROF link with DCM method, (a) DCM signal before transmission, (b) DCM signal arriving at the receiver, and (c) RF signal detected by the PD.

As we previously mentioned, PD is a squared-envelope operator, so the resulting signal satisfies the Equation (11):

$$|E_{rx2}(t)|^2 = \left\{\frac{m}{2} e^{j2\pi(f_c-f_m)t} + \left(\frac{m}{2}+1\right) e^{j(2\pi f_c t+\phi)} + \left(\frac{m}{2}+1\right) e^{j(2\pi(f_c+f_m)t+4\phi)} + \frac{m}{2} e^{j(2\pi(f_c+2f_m)t+9\phi)}\right\}.\left\{\frac{m}{2} e^{-j2\pi(f_c-f_m)t} + \left(\frac{m}{2}+1\right) e^{-j(2\pi f_c t+\phi)} + \left(\frac{m}{2}+1\right) e^{-j(2\pi(f_c+f_m)t+4\phi)} + \frac{m}{2} e^{-j(2\pi(f_c+2f_m)t+9\phi)}\right\} \quad (11)$$

By selecting only the component at frequency f_m, the desired signal can be obtained as:

$$|E_{rx2}(t)|^2 = \left(\frac{m}{2}\right)\left(\frac{m}{2}+1\right) e^{j(2\pi f_m t+\phi)} + \left(\frac{m}{2}+1\right)\left(\frac{m}{2}+1\right) e^{j(2\pi f_m t+3\phi)} + \left(\frac{m}{2}\right)\left(\frac{m}{2}+1\right) e^{j(2\pi f_m t+5\phi)}$$
$$|E_{rx2}(t)|^2 = e^{j2\pi f_m t}\left\{\left(\frac{m}{2}\right)\left(\frac{m}{2}+1\right) e^{j\phi} + \left(\frac{m}{2}+1\right)\left(\frac{m}{2}+1\right) e^{j3\phi} + \left(\frac{m}{2}\right)\left(\frac{m}{2}+1\right) e^{j5\phi}\right\} \quad (12)$$

Thus, the PD output RF signal has the equation

$$X_{rec2}(t) = \left\{\left(\frac{m}{2}\right)\left(\frac{m}{2}+1\right) e^{j\phi} + \left(\frac{m}{2}+1\right)\left(\frac{m}{2}+1\right) e^{j3\phi} + \left(\frac{m}{2}\right)\left(\frac{m}{2}+1\right) e^{j5\phi}\right\} \cos 2\pi f_m t \quad (13)$$

These three signals have phase differences, with RF signal II exhibiting the largest magnitude compared to RF signals I and III. RF signal I comes from the mixing process between OC1 and the lower sideband (LSB), RF signal II comes from the mixing between OC1 and OC2, and RF signal III comes from the mixing between OC2 and the upper sideband (USB). Although the three RF signals have different phases, only one dominant RF signal dominates, so the interference from these three signals becomes small, hence the system tends to remain stable and does not experience power fluctuations.

The amount of RF signal power generated by the PD can be calculated by squaring the amplitude part of equation (13). So that the amount of RF signal power output by the PD will fulfill equation (14),

$$P_{rec2}(t) = \left\{\left(\frac{m}{2}\right)\left(\frac{m}{2}+1\right)e^{j\phi} + \left(\frac{m}{2}+1\right)\left(\frac{m}{2}+1\right)e^{j3\phi} + \left(\frac{m}{2}\right)\left(\frac{m}{2}+1\right)e^{j5\phi}\right\}^2 \quad (14)$$

To test the effectiveness of this method in overcoming DPF, the RF signal power is calculated as a function of L using equation 14. The parameters used in this calculation are equalized with the previous calculation. The C/N penalty curve from this calculation is shown in Figure 7. From the figure, it can be seen that the power fluctuation is very small, and there is no deep fade as in the RoF system with direct modulation. The C/N deviation factor measurement result of this system shows a number of 1.13, proving that the DCM method can overcome DPF.

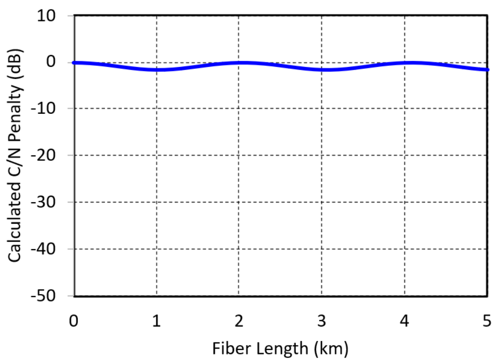

Figure 7. C/N Penalty curve calculated for RoF system with DCM method

C. RoF Simulation

To verify the effectiveness of DCM in mitigating DPF, RoF system measurements were conducted using a direct modulation scheme through simulations performed in OptiSystem software. The required data are acquired by recording the PD output RF power at varying fiber lengths (L). L s varied from 0 to 5 km in steps of 0.1 km, and f_m is set to 30 GHz, 40 GHz, and 60 GHz. The simulation circuit used in this study is shown in Figures 8 and 9.

The RoF simulation employing a direct modulation scheme is composed of several components: a Sine Generator, a Directly Modulated Laser Measured (DMLM), an Optical Fiber, a PIN Photodetector, a Band-Pass Rectangle Filter, an Optical Spectrum Analyzer (OSA), an RF Spectrum Analyzer, and an Electrical Power Meter (EPM). The Sine Generator provides a clean RF signal at 60 GHz, which is applied to the DMLM configured with the parameters listed in Table 1. The optical spectrum produced at the laser output is monitored using the OSA. The signal is subsequently propagated through a Single mode fiber (SMF). SMF parameters can be seen in Table 2. The effect of fiber attenuation is ignored in this simulation so that the influence of chromatic dispersion on the power of received RF can be clearly observed.

The optical signal at the receiver is transformed into an electrical signal using a PIN photodetector, configured with 1 A/W responsivity and 10 nA dark current. The photodetector output is then passed through a Band-Pass Rectangle Filter to suppress unwanted frequency components. The filter is configured with a 60 GHz center frequency, 40 MHz bandwidth, 0 dB insertion loss, and 100 dB depth to extract the desired RF signal. Finally, the power of received RF signal is evaluated using an EPM. The simulation circuit for DCM consists of components like the simulation circuit for ROF using the direct modulation scheme. However, in the Dual

Carrier ROF link, two Directly Modulated Laser Measured components with different frequencies are used. Since the f_m used is 60 GHz, Directly Modulated Laser Measured I is set with f = 193.414 THz, and Directly Modulated Laser Measured II is set with f = 193.474 THz. An OSA is used to observe the optical spectra of each carrier by connecting it to the outputs of the two Directly Modulated Lasers. Then, the two signals are combined using a power combiner (PC), and the combined signal spectrum shape is observed using an OSA. Transmission of the PC output is carried out via a Single-Mode Optical Fiber.

The optical signal at the receiver is detected by a PIN photodetector. A Band-Pass Rectangular Filter is employed to isolate the target RF signal frequency. The power of received RF signal is evaluated using an EPM.

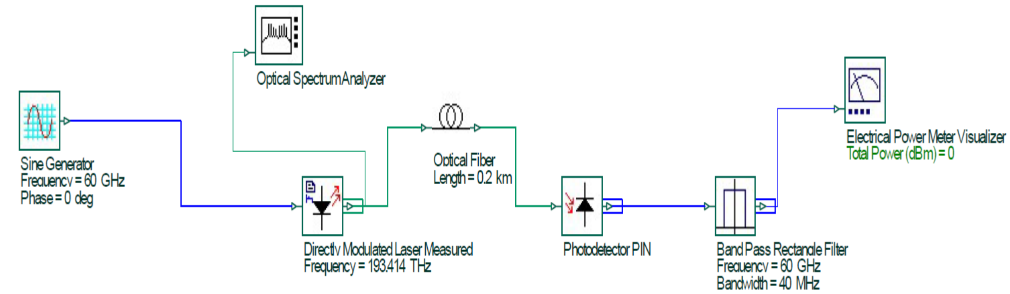

Figure 8. Simulation circuit of the ROF link with direct modulation scheme

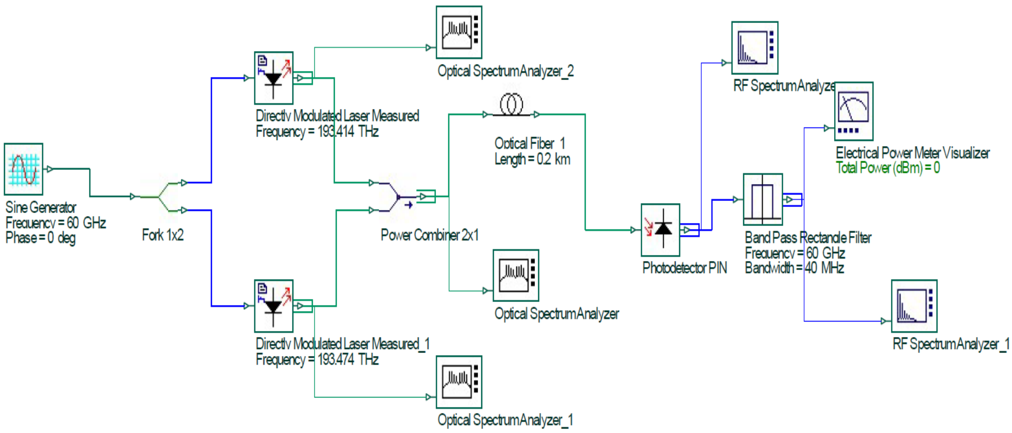

Figure 9. Simulation circuit of the ROF link with Dual Carrier Modulation scheme

Tabel 1. Setting parameter Directly Modulated Laser Measured

Parameter	Value	Units
Frequency	193.414	THz
Configuration	Analog	-
Power	10	dBm
Extinction ratio	10	dB
Threshold current	20	mA
Slope efficiency	0.4	W/A
Maximum current	300	mA
Linewidth	10	MHz
Initial phase	0	Deg

Table 2. Setting parameter Optical Fiber

Parameter	Value	Units
User defined reference wavelength	Checked	-
Reference wavelength	193.414	THz
Length	0 – 5	km
Attenuation effect	Unchecked	-
Group velocity dispersion	Checked	-
Third-order dispersion	Unchecked	-
Frequency domain parameter	Unchecked	-
Dispersion	17	ps/nm/km

3. Results and Discussion

A. Spectrum Shape

Figure 10 illustrates the output spectrum of the RoF simulation employing the direct modulation scheme, where the horizontal axis denotes frequency (Hz) and the vertical axis indicates power (dBm).

The figure shows that the RoF output spectrum under the direct modulation scheme exhibits a double sideband structure, with identical power levels for the upper and lower sidebands across all orders. In Figure 10a, it can be observed that the spectrum of the optical signal modulated by an RF signal with a frequency of 60 GHz has an optical carrier component with a frequency of 193.414 THz and frequencies of the upper and lower sidebands at 193.474 THz and 193.354 THz, respectively.

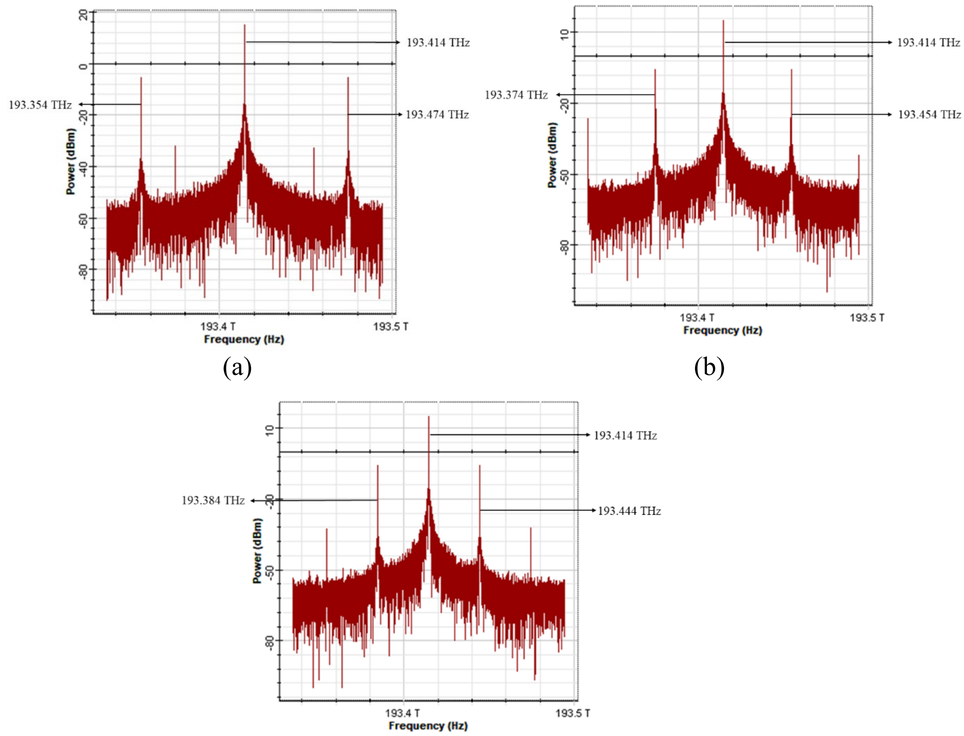

(a) (b)

(c)

Figure 10. Modulated optical signal spectrum with RF signal frequencies of (a) 60 GHz, (b) 40 GHz, and (c) 30 GHz

Figure 10b shows that for a 40 GHz RF modulation, the optical carrier, upper sideband, and lower sideband frequencies are 193.414 THz, 193.454 THz, and 193.373 THz, respectively. For a 30 GHz RF modulation (Figure 10c), the corresponding values are 193.414 THz, 193.444 THz, and 193.384 THz. These observations are consistent with theory, where the carrier-to-sideband spacing equals the modulating RF frequency.

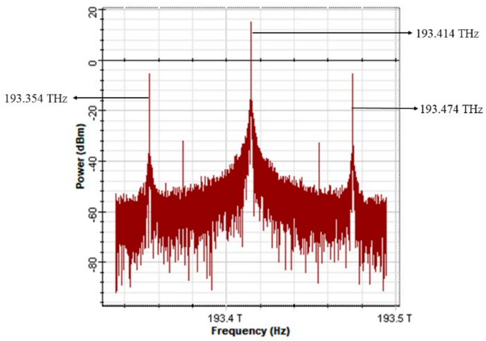

(a)

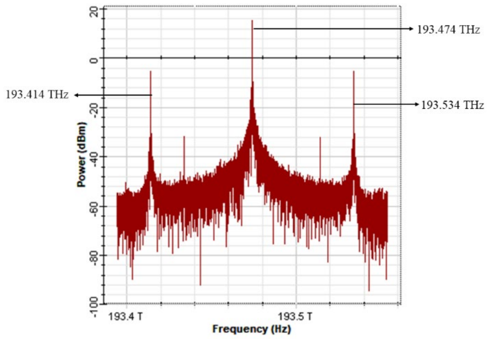

(b)

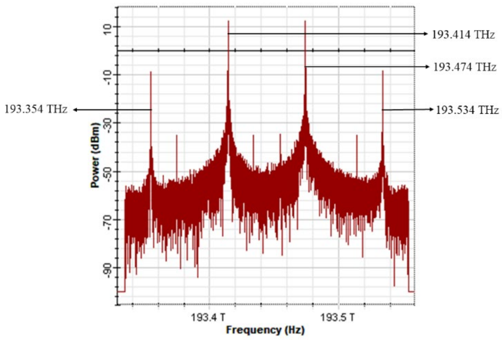

(c)

Figure 11. Optical signal spectrum with DCM method where (a) spectrum of the modulated optical signal I, (b) spectrum of the modulated optical signal II, and (c) spectrum of the optical signal in DCM form.

Figure 11 shows the output spectrum of DCM. As seen in Figure 11a, the spectrum of optical carrier 1 exhibits a double sideband structure, with the carrier, upper sideband, and lower sideband frequencies at 193.414 THz, 193.474 THz, and 193.354 THz, respectively. The spectrum of the optical signal generated by carrier 2 also exhibits a double sideband shape, but with the optical carrier frequency, upper sideband, and lower sideband frequencies being 193.474 THz, 193.534 THz, and 193.414 THz respectively, as seen in Figure 11b. The output spectrum after combining the two carriers will result in a spectrum like Figure 11c, which consists of two optical carriers with frequencies of 193.414 THz and 193.474 THz. The power of the upper and lower sidebands for all orders is the same. This proves that the modulator circuit designed to generate dual carrier modulation has functioned as expected.

B. DCM Performance

Figure 12a, b, and c respectively show the C/N Penalty of the simulated Double Sideband (DSB) ROF link and the DCM link with RF signal frequencies of 60, 40, and 30 GHz. The vertical axis in Figure 12 represents received RF signal Power (dBm), while the horizontal axis represents the fiber length (km).

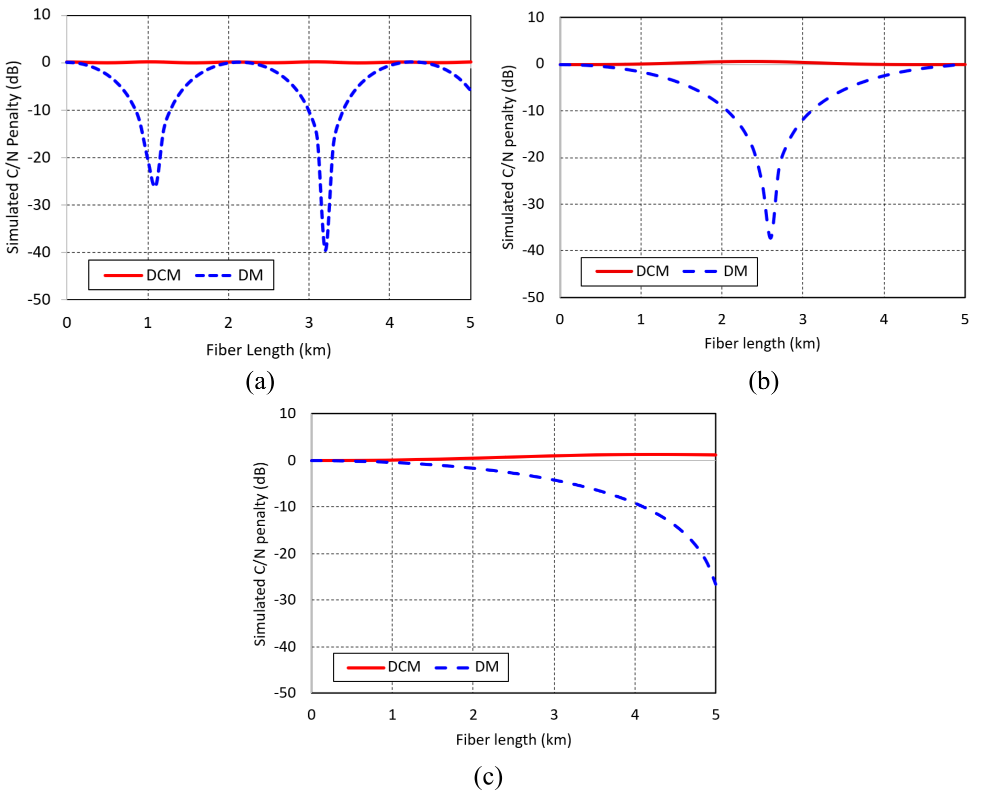

Figure 12. Simulation results of the RoF system with DM and DCM methods modulated by RF signals with frequencies of (a) 60 GHz, (b) 40 GHz, (c) 30 GHz.

Figure 12a shows that in the RoF system with direct optical modulation (DM), deep fade occurs at fiber lengths L = 1.1 and 3.2 km with a C/N deviation factor value of 7.59. As for the RoF system with the DCM method, no deep fade occurs with a C/N deviation factor value of 0.05. Figure 12b shows that in the RoF system with DM there is a deep fade at L = 2.6 km with a C/N deviation factor value of 7.63 while in the RoF system with the DCM method there is no deep fade where the C/N deviation factor value is 0.20. Figure 12c shows that in the RoF system with DM there is a deep fade at L around 5.1 km with a C/N deviation factor value of 6.30 while in the RoF system with the DCM method there is no deep fade with a C/N deviation factor value of 0.47. From these three figures, it can be said that the DCM method can overcome DPF at RF frequencies of 60, 40 and 30 GHz (different RF signal frequencies).

In previous research [5], simulations have been carried out to measure the performance of the RoF system with the OSSB method in overcoming DPF. The OSSB in the study was generated using a Dual-Drive Mach-Zehnder modulator (DD-MZM) which was given an RF signal input with a phase difference of 90°. From the research, it is known that the C/N deviation factor values for this RoF system when given RF signal input with frequencies of 60, 40 and 30 GHz are 0.9, 0.9 and 1.0. From this value, it can be seen that the RoF system with the DCM method can overcome DPF better than the OSSB method.

C. Comparison of DM and DCM Performance in Calculation and Simulation

The performance comparison between RoF systems using DM and DCM at a 60 GHz RF frequency, based on both simulation and calculation, is illustrated by the C/N penalty curve in Figure 13. From the figure, it can be observed that the C/N penalty curves from the simulation and calculation results have nearly identical shapes, although there is a slight discrepancy in the locations of the deep fades. This shows that the mathematical equations created to model the

RoF DM and DCM systems are correct. A comparison of the C/N penalty values at several deep fade points before and after applying the DCM method can be seen in Table 3.

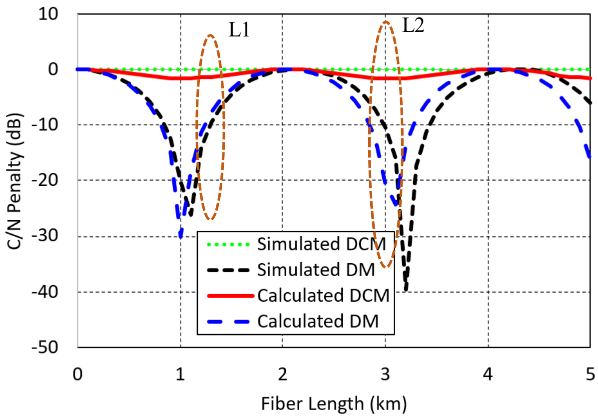

Figure 13. Comparison of calculated and simulated C/N penalty curves for RoF system with RF frequency of 60 GHz

Table. 3 Comparison of calculated and simulated C/N penalty values before and after applying the DCM method at several deep fade points for RoF system with 60 GHz RF frequency.

Length / Methode	C/N Penalty (dB)			
	L1		L2	
	DM	DCM	DM	DCM
Calculated	-30.15	-1.65	-24.33	-1.65
Simulated	-26.13	0.02	-39.63	0.02

From Table 3, it can be seen that when the DCM method is applied to the RoF system, the calculated C/N penalty value at the deep fade point L1 has increased from -30.15 dB to -1.65 dB. Simulation results also show an increase from -26.13 dB to 0.02 dB. At the deep fade L2 point, the calculated C/N penalty value also increased from -24.33 dB to -1.65 dB. The simulation results at this point also increased from -39.63 dB to 0.02 dB. This shows that the DCM method can overcome DPF in RoF systems.

The implementation of DCM offers clear advantages in mitigating dispersion-induced power fading. However, several trade-offs must also be considered to provide a balanced perspective. First, the use of two directly modulated lasers inevitably increases hardware requirements, including optical combining elements and additional power control circuitry. This added complexity may introduce extra cost and calibration effort, particularly in maintaining equal optical power levels and wavelength stability. Furthermore, DCM is inherently sensitive to relative phase and frequency alignment between the two optical carriers. Any phase drift or frequency offset can degrade the beating efficiency, leading to fluctuations in the recovered RF signal and potentially elevating the carrier-to-noise (C/N) penalty. In addition, the linewidth and relative intensity noise of both lasers may accumulate, further impacting performance if not properly managed. Despite these challenges, the trade-offs can be mitigated through practical techniques such as temperature stabilization, automatic power control, polarization-maintaining components, and lightweight digital phase-tracking schemes. When applied within these constraints, the additional overhead remains modest compared to the significantly higher complexity of OSSB or DD-MZM-based solutions. Thus, DCM represents a cost-effective and flexible approach, achieving a favorable balance between hardware simplicity and reliable dispersion compensation.

Table. 4 Comparison of key performace indicators

Technique	Complexity	Cost	Flexibility	Performance
OSSB	High (requires precise optical filtering)	High	Moderate	High spectral efficiency, but sensitive to filter imperfections
OCS	Low (simple modulation structure)	Low	Low	Limited dispersion tolerance, lower spectral efficiency
CPS	Moderate (requires phase control circuitry)	Moderate	Moderate	Improved dispersion tolerance, but higher implementation effort
DD-MZM	High (dual-drive Mach–Zehnder)	High	Moderate	High performance and dispersion resilience, but expensive and complex
DCM (Proposed)	Low–Moderate (only two directly modulated lasers required)	Low–Moderate	High (simple setup, scalable)	Good balance between complexity and dispersion compensation

Finally, Table 4 presents a performance comparison, showing that DCM achieves a favorable balance between implementation complexity and dispersion compensation. By requiring only two directly modulated lasers, DCM provides lower cost and higher flexibility compared to conventional approaches, while still ensuring effective mitigation of dispersion-induced impairments.

4. Conclusion

This study employs the DCM method to mitigate dispersion power fading (DPF) in RoF links. For the 60 GHz RoF link using direct modulation (DM), a notable power reduction occurs at fiber lengths of 1.1 km and 3.2 km, with a C/N deviation factor of 7.59. In the RoF link with direct modulation at 40 GHz, a significant power drop occurs at a fiber length of 2.6 km, corresponding to a C/N deviation factor of 7.63. At 30 GHz, a similar power drop occurs around 5.1 km, with a C/N deviation factor of 6.30. From the power measurements over a fiber length range of 0 to 5 km, the power curve generated by DCM remains stable without any deep fades. The C/N deviation factor values for this system at 60, 40, and 30 GHz are 0.05, 0.20, and 0.47, respectively. Therefore, the simulation results demonstrate that the DCM method can effectively mitigate DPF.

5. Acknowledgment

This research received funding from Penelitian Fundamental Reguler, DRTPM, Kementerian Pendidikan Tinggi, Sains, dan Teknologi (Kemdiktisaintek). Indonesia.

References

[1]. N. I. Andrikogiannopoulos, "RF phase modulation of optical signals and optical/electrical signal processing," Massachusetts Institute of Technology, 2006.
[2]. X. N. Fernando, *Radio over fiber for wireless communications: from fundamentals to advanced topics*. John Wiley & Sons, 2014.
[3]. U. Gliese, S. Norskov, and T. Nielsen, "Chromatic dispersion in fiber-optic microwave and millimeter-wave links," *IEEE Transactions on microwave theory and techniques,* vol. 44, no. 10, pp. 1716-1724, 2002.
[4]. I. G. Insua, *Optical generation of mm-wave signals for use in broadband radio over fiber systems*. Jörg Vogt Verlag, 2010.

[5]. F. Ujang, T. Firmansyah, P. S. Priambodo, and G. Wibisono, "Irregular shifting of RF driving signal phase to overcome dispersion power fading," *Photonics,* vol. 6, no. 4, p. 104, 2019.
[6]. M. Yuan *et al.*, "Broadband Microwave Photonic Mixer with Flexibly Tunable Phase Shift and Supporting Dispersion-Induced Power-Fading-Free Fiber Transmission," *Photonics,* vol. 10, no. 4, p. 432, 2023.
[7]. C. Yin *et al.*, "Microwave photonic frequency up-convertor with frequency doubling and compensation of chromatic-dispersion-induced power fading," *IEEE Photonics Journal,* vol. 9, no. 3, pp. 1-7, 2017.
[8]. Z. Dong, "64QAM vector radio-frequency signal generation based on phase precoding and optical carrier suppression modulation," *IEEE Photonics Journal,* vol. 8, no. 6, pp. 1-7, 2016.
[9]. Z. Jia, J. Yu, and G.-K. Chang, "A full-duplex radio-over-fiber system based on optical carrier suppression and reuse," *IEEE Photonics Technology Letters,* vol. 18, no. 16, pp. 1726-1728, 2006.
[10]. Y. Tian, K.-L. Lee, C. Lim, and A. Nirmalathas, "Experimental comparison of DSB-SC & OSSB based 60 GHz radio-over-fiber fronthaul links," in *2016 IEEE International Topical Meeting on Microwave Photonics (MWP)*, 2016: IEEE, pp. 141-144.
[11]. N. A. Al-Shareefi *et al.*, "A study in OCS millimeter-wave generation using two parallel DD-MZMs," in *2013 IEEE 11th Malaysia International Conference on Communications (MICC)*, 2013: IEEE, pp. 418-421.
[12]. F. Ujang *et al.*, "Eliminating Dispersion Power Fading in Radio over Fiber Communication through Unbalanced Sideband Modulation [J]," *International Journal of Electrical and Electronic Engineering & Telecommunications,* vol. 13, no. 6, pp. 456-466, 2024.
[13]. H. Kressel, M. Ettenberg, J. Wittke, and I. Ladany, "Laser diodes and LEDs for fiber optical communication," in *Semiconductor devices for optical communication*: Springer, 2005, pp. 9-62.
[14]. G. P. Agrawal, *Fiber-optic communication systems*. John Wiley & Sons, 2012.
[15]. S. Santhanam and T. K. M. Selvi, "Radio Over Fiber Technologies of Wireless Broadband Access Network," in *2024 3rd International Conference on Applied Artificial Intelligence and Computing (ICAAIC)*, 2024: IEEE, pp. 1629-1635.

Febrizal Ujang was born in Selatpanjang, Indonesia. He earned a Bachelor's degree in Electrical Engineering in 2002 from the University of North Sumatra and a Master's degree in Telecommunication Engineering in 2009 from the Bandung Institute of Technology. He has been a lecturer and researcher at the University of Riau since 2003. He earned a Doctorate in Electrical Engineering in 2021 from the University of Indonesia. His research interests include wireless communications, IoT, and optical communications.

Muhammad Firdaus was born in Kateman, Indragiri Hilir, Indonesia, in 2002. He is currently pursuing a B.Eng. degree in Electrical Engineering at Universitas Riau. Beyond academics, he enjoys music and sports. Following graduation, he plans to continue advanced studies in electronics and optical communications with the aim of making meaningful contributions to the field.

Ken Paramayudha earned his Bachelor of Electrical Engineering in 2009 from the Bandung Institute of Technology, Indonesia, and his Master of Philosophy in Electrical and Electronic Engineering in 2019 from the University of Adelaide, Australia. He has been a Research Assistant at PPET-LIPI since 2014. His research interests include reconfigurable antennas and microwave devices. He was a finalist for the Best Student Paper Award at the 2018 Australian Microwave Symposium and won the Best Poster Presentation Award at the 2019 Indonesia–Japan Wireless Antenna and Technology Workshop.

Teguh Firmansyah was born in Subang, Indonesia. He earned his Bachelor of Engineering (S.Eng.) and Master of Engineering (M.Eng.) degrees in Electrical Engineering from the University of Indonesia in 2010 and 2012, respectively, and earned his Dr.Eng. degree in 2022 from Shizuoka University, Japan. He has been a Lecturer at Sultan Ageng Tirtayasa University since 2012. He holds two patents related to broadband and multiband antennas. His research focuses on microwave circuit design for various applications and the development of multifunctional sensors using acoustic, plasmonic, and microwave resonators.